

Published in final edited form as:

Curr Biol. 2012 June 5; 22(11): 956–966. doi:10.1016/j.cub.2012.03.068.

PTK7 regulates myosin II activity to orient planar polarity in the mammalian auditory epithelium

Jianyi Lee¹, Anna Andreeva¹, Conor W. Sipe¹, Lixia Liu^{1,2}, Amy Cheng^{1,3}, and Xiaowei Lu¹

¹Department of Cell Biology, P.O. Box 800732, University of Virginia, Charlottesville, VA 22908, USA

Summary

Background—Planar Cell Polarity (PCP) signaling is a key regulator of epithelial morphogenesis, including neural tube closure and the orientation of inner ear sensory hair cells, and is mediated by a conserved noncanonical Wnt pathway. *Ptk7* is a novel vertebrate-specific regulator of PCP, yet the mechanisms by which *Ptk7* regulates mammalian epithelial PCP remain poorly understood.

Results—Here we show that, in the mammalian auditory epithelium, *Ptk7* is not required for membrane recruitment of Dishevelled 2; *Ptk7* and *Frizzled3/Frizzled6* receptors act in parallel and have opposing effects on hair cell PCP. Mosaic analysis identified a requirement of *Ptk7* in neighboring supporting cells for hair cell PCP. *Ptk7* and the noncanonical Wnt pathway differentially regulate a contractile myosin II network near the apical surface of supporting cells. We provide evidence that this apical myosin II network exerts polarized contractile tension on hair cells to align their PCP, as revealed by asymmetric junctional recruitment of vinculin, a tension-sensitive actin binding protein. In *Ptk7* mutants, compromised myosin II activity resulted in loss of planar asymmetry and reduced junctional localization of vinculin. By contrast, vinculin planar asymmetry and stereociliary bundle orientation were restored in *Fz3^{-/-}; Ptk7^{-/-}* double mutants.

Conclusions—These findings suggest that PTK7 acts in conjunction with the noncanonical Wnt pathway to orient epithelial PCP through modulation of myosin-II based contractile tension between supporting cells and hair cells.

Keywords

PTK7; Frizzled3; non-muscle myosin II; vinculin; planar cell polarity; sensory hair cells; supporting cells; contractile tension

Introduction

Epithelial cells are often polarized within the plane of a cell sheet, perpendicular to the apical-basal polarity axis. One of the most prominent examples of epithelial planar cell polarity (PCP) is found in the mammalian auditory sensory epithelium, the organ of Corti (OC). The OC is composed of one row of inner hair cells (IHC) and three rows of outer hair cells (OHC) and non-sensory supporting cells. Hair cells are separated from one another by

¹Corresponding Author: Xiaowei Lu, Department of Cell Biology, University of Virginia, P.O. Box 800732, Charlottesville, Virginia 22908 Ph: 434-982-6528; Fax: 434-982-3912; xl6f@virginia.edu.

²Present address: Department of Medicine, Allergy and Immunology, P.O. BOX 800133, University of Virginia, Charlottesville, VA 22908, USA

³Present address: Georgetown University School of Medicine, Washington, DC 20057

The authors declare no competing financial interests.

supporting cells, forming a checkerboard pattern. The stereociliary bundle, the mechanotransduction organelle located on the apical surface of the hair cell, consists of rows of actin-based stereocilia of graded heights in a V-shaped array. This structural asymmetry of the stereociliary bundle defines PCP of an individual hair cell. Across the OC, hair cells display uniform planar polarity, with the vertex of their V-shaped stereociliary bundles all pointing to the lateral edge of the cochlear duct. Uniform bundle orientation is required for normal sound perception [1].

Inner ear PCP is regulated by an evolutionarily conserved noncanonical Wnt pathway, which has emerged as a key regulator of metazoan tissue morphogenesis, including convergent extension (CE) movements during axis elongation, neural tube closure and inner ear morphogenesis [2]. The core components of the noncanonical Wnt pathway are Frizzled (Fz), Dishevelled (Dsh/Dvl), Strabismus (Stbm)/Van Gogh (Vang), Starry night (Stan)/Flamingo (Fmi), Diego (Dgo) and Prickle (Pk). These molecules engage in both intra- and inter-cellular signaling to align PCP in neighboring cells. In other systems, members of the Rho family small GTPases (RhoA, Rac1 and Cdc42) and their effectors, including Rho-associated kinases (ROCK) and c-Jun N-terminal kinases (JNK), have been implicated in PCP signaling downstream of the core components. In the inner ear, the noncanonical Wnt pathway is required for stereociliary bundle orientation and cochlear convergent extension [3]. Mutations in homologs of Fmi (Celsr1), Vang (Vangl1/Vangl2), Fz (Fz2/Fz3/Fz6) and Dsh (Dvl1/Dvl2/Dvl3) cause misoriented stereociliary bundles and a shortened cochlear duct [2]. The small GTPase Rac1 and its downstream effector p21-activated kinases (PAK) regulate hair cell PCP in the OC [4, 5], while non-muscle myosin II has been implicated in cochlear extension [6].

In addition to the conserved noncanonical Wnt pathway, novel PCP regulators have been identified in mammals, including *Protein tyrosine kinase 7 (Ptk7)*, a receptor tyrosine kinase-like molecule [7–11]. Mouse *Ptk7* mutations cause similar phenotypes to those of noncanonical Wnt pathway mutants, including neural tube and hair cell PCP defects [8, 12]. In *Xenopus*, *Ptk7* has been shown to regulate neural tube closure [8] and neural crest migration [13, 14] by mediating membrane recruitment of Dishevelled through PKC δ and the adaptor molecule RACK1 [13, 14]. However, it is unclear whether PTK7 regulates mammalian epithelial PCP by a similar mechanism, as PTK7 has been shown to mediate mesodermal CE in mice without affecting Dvl2 membrane localization [15].

To gain insight into the mechanisms by which PTK7 regulates mammalian epithelial PCP, we carried out a functional dissection of *Ptk7* in planar polarization of hair cells in the OC, where bundle orientation provides a robust and quantifiable readout for PCP at single-cell resolution. Our results reveal that *Ptk7* and the noncanonical Wnt pathway differentially regulate myosin II-based contractility to align hair cell PCP. We show that *Ptk7* is required in supporting cells to orient hair cell PCP, likely by exerting contractile tension on neighboring hair cells through an apical myosin II network.

Results

Ptk7 is not required for asymmetric membrane localization of Dishevelled-2 in the OC

Membrane recruitment and asymmetric localization of the cytoplasmic scaffold protein Dishevelled is a conserved readout for PCP signaling [16–18]. To determine where *Ptk7* intersects with the noncanonical Wnt pathway, we first tested if *Ptk7* is required for membrane recruitment of Dvl2. At E17.5, in the mid-basal region of control OC, endogenous Dvl2 is asymmetrically localized and appears to be enriched on the lateral membranes of hair cells (Figure 1A, C). Dvl2 localization is disrupted in *Vangl2^{Lp/Lp}* OC [18] and *Fz3^{-/-}; Fz6^{-/-}* OC (Supplemental Figure S1), indicating that Dvl2 localization is a

functional readout of the noncanonical Wnt pathway activity. By contrast, Dvl2 localization was normal in the *Ptk7*^{-/-} OC at E17.5 (Figure 1B, D). Similarly, in the mid-apical region of OC, membrane recruitment of Dvl2 occurred in both control and *Ptk7*^{-/-} OC (Figure 1E–H). We also examined Fz3 localization at E17.5, which is normally enriched along the medial poles of hair cells and supporting cells [19, 20] (Figure 1I, K, M, O). Interestingly, membrane localization of Fz3 was significantly reduced in the *Ptk7*^{-/-} OC (Figure 1J, L, N, P). These results indicate that *Ptk7* regulates Fz3 localization but is not required for asymmetric membrane localization of Dvl2 in the OC. Thus, the noncanonical Wnt pathway is at least partially active in the absence of *Ptk7*.

PTK7 and Fz3/Fz6 receptors act in parallel and have opposing effects on hair cell PCP

The normal Dvl2 membrane localization and reduced Fz3 localization in *Ptk7*^{-/-} OC suggests that *Ptk7* is not an obligatory component of the noncanonical Wnt pathway, however it may regulate the strength of noncanonical Wnt signaling. To test this idea, we next sought to determine the epistatic relationship between *Ptk7* and the *Fz3/6* genes. Mouse *Fz3* and *Fz6* regulate PCP signaling in a redundant manner [19]. We used bundle orientation as readout for PCP, which is already evident at embryonic day (E) 18.5. In the control, the vertices of the V-shaped stereociliary bundles all point toward the lateral edge of the cochlear duct (Figure 2A, A'). While *Fz3* or *Fz6* single mutants had normal bundle orientation (Figure 2B, B' and data not shown), *Fz3*^{-/-}; *Fz6*^{-/-} mutants had misoriented stereociliary bundles, affecting primarily IHCs [19] (Figure 2C, C', Supplemental Figure S2). By contrast, in the *Ptk7*^{-/-} OC, bundle misorientation was confined to OHC3 (Figure 2D, D', Supplemental Figure S2). Surprisingly, bundle misorientation in OHC3 was significantly suppressed in both *Fz3*^{-/-}; *Ptk7*^{-/-} and *Fz6*^{-/-}; *Ptk7*^{-/-} mutants (Figure 2E, E' and data not shown). These results indicate that *Ptk7* and *Fz3/Fz6* have opposing effects on hair cell PCP and suggest that *Ptk7* acts upstream of or in parallel to *Fz3/Fz6*. To distinguish between these two possibilities, we analyzed bundle orientation in *Fz3*^{-/-}; *Fz6*^{-/-}; *Ptk7*^{-/-} triple mutants. If *Ptk7* acts upstream of *Fz3/Fz6* in a linear genetic pathway, then the *Fz* mutations should be epistatic to *Ptk7*, i.e. the triple mutants should have a phenotype similar to *Fz3/Fz6* double mutants. On the other hand, if *Ptk7* acts in parallel to *Fz3/Fz6*, then neither mutation should be epistatic; instead, the triple mutants may show an additive phenotype. Indeed, the triple mutants displayed a combination of the *Fz3/Fz6* and *Ptk7* mutant phenotypes: both IHC and OHC rows displayed misoriented stereociliary bundles (Figure 2F, F', Supplemental Figure S2). Taken together, these results indicate that *Ptk7* and *Fz3/Fz6* act in parallel and have opposing effects on hair cell PCP.

PTK7 is required in supporting cells to regulate hair cell PCP

Next, we sought to determine the site of action of *Ptk7* in the OC. To this end, we generated a 'floxed' allele of *Ptk7* (*Ptk7*^{CO}). A knock-out allele (*Ptk7*⁻) was derived from *Ptk7*^{CO} upon germline Cre expression (Supplemental Figure S3A, B). We first used the *Foxg1*^{Cre} line [21] to inactivate *Ptk7* in the entire cochlear epithelium. OHC3s in these mutants displayed misoriented stereociliary bundles similar to *Ptk7*^{-/-} mutants (Supplemental Figure S3C–E), indicating that *Ptk7* acts within the cochlear epithelium to regulate hair cell PCP.

We then carried out genetic mosaic analysis to further determine the cell-type specific requirement of *Ptk7*. PTK7 is expressed in both hair cells and supporting cells and co-localizes with the adherens junction protein E-cadherin [8] (Figure 3B). To generate *Ptk7* mosaics, we took advantage of the *EIIa-Cre* line [22], which expresses Cre in all cells but at variable levels. In *EIIa-Cre*; *Ptk7*^{CO/-} animals, cells with high Cre expression level would have a genotype of *Ptk7*^{-/-}, while cells with low Cre expression level would have a genotype of *Ptk7*^{CO/-} thus retaining a functional copy of *Ptk7* (referred to as *Ptk7*⁺ thereafter). The genotypes of individual cells in the OC were unambiguously determined by

the presence or absence of PTK7 immunostaining (Figure 3B–F). Because only OHC3s were affected in *Ptk7* mutants, we focused on OHC3s and correlated bundle orientation with the genotypes of each hair cell and its four immediate supporting cell neighbors (Figure 3A, shaded in blue). Many mosaics had a *Ptk7*⁺ hair cell with a misoriented stereociliary bundle surrounded by varying numbers of *Ptk7*^{-/-} supporting cells (arrows, Figure 3C–F’). Moreover, as the number of *Ptk7*^{-/-} supporting cells surrounding a *Ptk7*⁺ hair cell increased (up to 4), both the penetrance and the severity of bundle misorientation defect increased (Figure 3G, H). Together, these results indicate that *Ptk7* function in hair cells alone is insufficient for normal bundle orientation, and that *Ptk7* is required in supporting cells to regulate hair cell PCP.

JNK signaling is unlikely to mediate PTK7 function in the OC

Our results so far are consistent with a model where *Ptk7* and the noncanonical Wnt pathway converge on common effectors to regulate bundle orientation. It has been shown that the noncanonical Wnt pathway activates JNK signaling in other systems [23, 24]. We therefore considered the possibility that *Ptk7* has an opposing effect on Fz-mediated JNK signaling. To test this, we performed biochemical assays for JNK activation in HEK293T cells (Figure 4A). Using phosphorylation of c-Jun as readout, we found that expression of PTK7 alone had a minimal effect on JNK activation, while expression of Fz3 alone led to JNK activation. Moreover, coexpression of PTK7 and Fz3 did not inhibit JNK activation by Fz3. Thus, in this heterologous system, there was no apparent effect of PTK7 on JNK signaling.

Next, we examined if PTK7 regulates JNK signaling *in vivo*. Using antibodies that specifically recognize phosphorylated and activated JNK (pJNK), we found that, in E17.5 controls, pJNK localized to cellular junctions and the tips of a subset of stereocilia (Figure 4B–B’), suggesting JNK signaling is active during cochlear morphogenesis. However, in *Ptk7*^{-/-} OC, we did not observe any significant changes in pJNK levels or localization (Figure 4C–C’), suggesting that JNK is unlikely to be a downstream effector of PTK7 in the OC.

To more rigorously assess if PTK7 regulates inner ear PCP through JNK signaling, we next examined genetic interactions between *Ptk7* and the *Jnk* genes using bundle orientation as readout. Among the three mouse homologs of *Jnk*, *Jnk1* and *Jnk2* are broadly expressed. While single *Jnk* knock-out mice are viable, *Jnk1/2* double mutants display neural tube defects and die at E10.5 [25–27]. We found that *Jnk1* and *Jnk2* single mutants had essentially normal bundle orientation at E18.5 (Figure 4E and data not shown). In the *Jnk1*^{-/-}; *Ptk7*^{-/-} OC, bundle misorientation persisted in OHC3s, comparable in severity to *Ptk7*^{-/-} mutants (Figure 4F). Similar results were obtained in *Jnk2*^{-/-}; *Ptk7*^{-/-} double mutants (data not shown). Therefore, unlike *Fz3/Fz6* mutations, *Jnk1/Jnk2* mutations had no effect on the bundle misorientation phenotype of *Ptk7* mutants, providing further evidence that JNK is unlikely to mediate PTK7 signaling in the OC.

Ptk7 and the noncanonical Wnt pathway differentially regulate a contractile apical myosin II network in supporting cells

To further pursue downstream effectors of *Ptk7*, we next investigated a potential role of *Ptk7* in regulating myosin II function in the OC. It has been shown that noncanonical Wnt signaling activates actomyosin contractility in other systems [28–30]. Moreover, myosin II regulates CE and neural tube closure in *Xenopus* [31, 32] and cochlear extension in mice [6].

We first examined myosin IIB (MIIB, encoded by *Myh10*), one of the three myosin II heavy chain proteins (MIIA, MIIB and MIIC) expressed during cochlear morphogenesis [6]. Hair cell planar polarization and stereociliary bundle formation proceed in a base-to-apex gradient starting at the base of the cochlea around E16.5, as evidenced by migration of the axonemal kinocilium [7] and asymmetric localization of activated PAK [4]. At E16.5, in control tissues, MIIB was localized to cellular junctions [6] (Figure 5A–E). In addition, in the mid-basal region of the cochlea, we also observed an assembly of MIIB foci near the apical surface of supporting cells (pillar and Deiters' cells) (Figure 5A–C, arrows). By contrast, the apical MIIB foci were absent from the supporting cells in the mid-basal region of the *Ptk7*^{-/-} OC and overall junctional localization of MIIB was reduced compared to controls (Figure 5F–J). Western blot analysis of E16.5 cochlear lysates showed that total levels of MIIB in *Ptk7*^{-/-} cochleae were similar to controls (Figure 5K). These results indicate that *Ptk7* promotes junctional localization of MIIB and is required for the assembly of apical MIIB foci in supporting cells.

To determine if the noncanonical Wnt pathway also regulates MIIB localization, we examined *Fz3*^{-/-}; *Fz6*^{-/-} and *Vangl2*^{Lp/Lp} cochleae at E16.5. In contrast to *Ptk7* mutants, the apical MIIB foci still formed in the supporting cells of *Fz3*^{-/-}; *Fz6*^{-/-} and *Vangl2*^{Lp/Lp} mutants, albeit smaller in size compared to controls (Figure 5L–O). Interestingly, junctional MIIB levels were significantly reduced in *Vangl2*^{Lp/Lp} mutants (Figure 5N, O) but only slightly reduced in *Fz3*^{-/-}; *Fz6*^{-/-} mutants (Figure 5L, M). Thus, *Ptk7* and the noncanonical Wnt pathway differentially regulate MIIB localization in the OC.

We next asked if the apical MIIB foci in supporting cells were contractile structures. Because force generation by myosin II molecules requires their ATPase activity [33], we reasoned that formation of an active contractile network should be disrupted upon inhibition of the myosin ATPase activity. To test this hypothesis, we took advantage of a Cre-inducible dominant-negative allele of *Myh10* (*Myh10*^{DN}) carrying a point mutation (R709C) in MIIB, which retains actin binding but compromises the actin-activated ATPase activity [34]. *Foxg1*^{Cre} was used to activate the expression of MIIB (R709C) in the cochlear epithelium, such that *Foxg1*^{Cre}; *Myh10*^{DN/DN} animals expressed only mutant (R709C) MIIB in the cochlea. Immunostaining revealed that MIIB (R709C) was still localized to cellular junctions but failed to assemble into apical foci in supporting cells at E16.5 (Figure 5R–S). These observations indicate that assembly of apical MIIB foci requires its ATPase activity and strongly suggest that the apical MIIB foci in supporting cells are contractile structures.

Ptk7 regulates myosin II activity to orient hair cell PCP

Decreased junctional MIIB level and the absence of apical MIIB foci in the *Ptk7*^{-/-} OC suggest compromised myosin II activity. Myosin II is activated by myosin regulatory light chain (RLC) phosphorylation, which is required for actomyosin contractility [33]. We therefore examined the distribution of phosphorylated RLC (pRLC) in the OC. At E16.5, in the mid-basal region of the control OC, pRLC was primarily detected at cellular junctions with higher intensity around pillar cell membranes (Figure 6A, B). In E16.5 *Ptk7*^{-/-} OC, pRLC staining appeared to be decreased at cell-cell contacts compared to controls, but, surprisingly, it was highly localized to apical foci in supporting cells (Figure 6C, D, arrows). By Western blot analysis, *Ptk7*^{-/-} cochleae showed a ~2-fold increase in total pRLC levels compared to controls (Figure 6M).

The paradox of the absence of MIIB and increased staining of pRLC in apical foci in *Ptk7*^{-/-} supporting cells suggests that other myosin II heavy chain molecules may be present in these structures. We therefore examined MIIC and MIIA distribution in *Ptk7*^{-/-} OC. In the mid-basal region of the control OC at E16.5, both MIIC and MIIA were detected at apical foci in supporting cells (Figure 6E, F, I, J). Overall, MIIC appeared to be enriched in supporting

cells, whereas MIIA localization was diffused and hardly detectable at cell boundaries. In *Ptk7*^{-/-} OC, MIIC staining appeared to be decreased at cell-cell contacts but was still present at apical foci in supporting cells (Figure 6G, H), whereas MIIA staining at apical foci in supporting cells was greatly reduced (Figure 6K, L). Western blot analysis showed that in *Ptk7*^{-/-} cochleae, total levels of MIIC were slightly increased (Figure 6N), while total MIIA levels were similar compared to controls (Figure 6O). Taken together, reduced junctional localization of MIIB, MIIC and pRLC and the absence of MIIB and MIIA in apical foci in *Ptk7*^{-/-} OC suggest that *Ptk7* regulates myosin II activity.

If compromised myosin II activity caused bundle misorientation in *Ptk7*^{-/-} mutants, then blocking myosin II activity should result in similar bundle orientation defects. Because MIIA, MIIB and MIIC are all present and likely function redundantly in the OC, we took a pharmacological approach and applied the myosin II inhibitor blebbistatin to cochlear explant cultures around the time of stereociliary bundle formation (Supplemental Experimental Procedures). We found that explants treated with blebbistatin displayed bundle misorientation (arrows, Figure 6Q), whereas bundle orientation in control explants was relatively normal (Figure 6P). Therefore, we conclude that myosin II activity is required for hair cell PCP.

Ptk7 promotes planar asymmetry of junctional vinculin

Defects in myosin II localization suggest that myosin II function is compromised in *Ptk7*^{-/-} OC. To evaluate myosin II function, we examined junctional vinculin localization. Vinculin is a tension-sensitive actin-binding protein involved in anchoring actin filaments to adhesion complexes at both focal adhesions and adherens junctions [35–37]. Recent *in vitro* studies demonstrate that recruitment of vinculin to adhesion sites is myosin II-dependent [38–41]. At E16.5, we observed a base-to-apex gradient of junctional vinculin localization in the control OC that coincides with the gradient of MIIB distribution (see Figure 5A–E). In the mid-basal region of control cochlea, vinculin was asymmetrically localized along cell-cell contacts and enriched on the medial side of hair cell membranes (Figure 7A–C). Strikingly, in the mid-basal region of the *Ptk7*^{-/-} OC, planar asymmetry of junctional vinculin was abolished, and overall junctional vinculin staining was reduced compared to controls (Figure 7D–F). On the other hand, localization of resident adherens junction proteins, including E-cadherin and β -catenin, was comparable to controls (Supplemental Figure S4), suggesting that loss of vinculin planar asymmetry in *Ptk7*^{-/-} OC is not a result of disrupted adherens junctions. In the apex, junctional vinculin staining in control and *Ptk7*^{-/-} OC was similar and both lacked apparent planar asymmetry (Figure 7G–J). These results indicate that *Ptk7* promotes planar asymmetry of junctional vinculin and strongly support the hypothesis that *Ptk7* regulates myosin II-based polarized contractile forces between OC epithelial cells.

Planar asymmetry of junctional vinculin is restored in *Fz3*^{-/-}; *Ptk7*^{-/-} mutants

In *Ptk7* mutants, loss of vinculin planar asymmetry correlated with bundle misorientation. To further understand the functional significance of vinculin planar asymmetry as well as the basis for the suppression of the *Ptk7* bundle orientation phenotype by *Fz3* (see Figure 2), we examined vinculin localization in *Fz3*^{-/-} and *Fz3*^{-/-}; *Ptk7*^{-/-} mutants at E16.5. In the *Fz3*^{-/-} OC, staining intensity of junctional vinculin was similar to controls, though its planar asymmetry appeared less robust (Figure 7K–M). Remarkably, planar asymmetry of junctional vinculin was restored in *Fz3*^{-/-}; *Ptk7*^{-/-} mutants (Figure 7N–P). Moreover, *Fz3*^{-/-}; *Ptk7*^{-/-} double mutants showed an increase in junctional MIIB levels and reappearance of apical MIIB foci in supporting cells compared to *Ptk7* single mutants (Supplemental Figure S4). Taken together, these results demonstrate a strong correlation between vinculin planar asymmetry and hair cell PCP, and further suggest that *Ptk7* and *Fz3* act in an opposing fashion to regulate contractile forces between OC epithelial cells.

Discussion

In this study, we present multiple lines of evidence that *Ptk7* is not an obligatory component of the noncanonical Wnt pathway; rather, during PCP signaling in the auditory epithelium, *Ptk7* and the noncanonical Wnt pathway differentially regulate myosin II-based contractile forces to orient PCP. Furthermore, we uncover an active role of supporting cells in this process through a contractile apical myosin II network (Figure 7Q).

In the mouse, *Ptk7* is not required for membrane recruitment of Dvl2 either in the inner ear (this study) or in the mesoderm during gastrulation [15]. These results contradict studies in *Xenopus*, where it has been shown that *Ptk7* mediates membrane recruitment of Dishevelled through a PKC δ -dependent mechanism [13, 14]. A possible explanation is that the *Xenopus* Dishevelled membrane recruitment assay was based on exogenously expressed Dishevelled, while we examined endogenous Dvl2 in the mouse. There is also evidence that PTK7 may have evolved different functions in mice and *Xenopus*. For example, PTK7 has been shown to regulate neural crest migration in *Xenopus*, but not in mice [12, 13]. While it is formally possible that PTK7 might mediate membrane localization of other mouse Dishevelled proteins (Dvl1 and Dvl3), it is unlikely to be the primary function of PTK7 in PCP regulation in the OC. Instead, our results strongly support a function of PTK7 in myosin II regulation to align PCP.

Interestingly, bundle misorientation in *Ptk7* mutants is largely restricted to OHC3 despite broad expression of PTK7 in the cochlea. OHC3s are positioned at the lateral edge of the OC and, as such, are mechanically coupled to a different group of cells than the other hair cell rows. We speculate that their unique mechanical environment may render OHC3s more sensitive to compromised myosin II function in *Ptk7* mutants. Furthermore, normal Dvl2 localization suggests that the noncanonical Wnt pathway is at least partially active in *Ptk7* mutants. We propose that overall PCP signaling is weakened but not disrupted in *Ptk7* mutants, resulting in defects only in OHC3s.

Our genetic analysis revealed, rather surprisingly, opposing effects of *Ptk7* and *Fz3/Fz6* on stereociliary bundle orientation. These findings contrast with our earlier observation that *Ptk7* and *Vangl2^{L-P}* mutations showed a positive genetic interaction such that double heterozygous animals displayed spina bifida [8]. It is worth noting that an allelic series of *Vangl2* mutations caused neural tube defects ranging from mild (e.g. spina bifida) to severe (e.g. craniorachischisis) in both mice and humans [42–44]. Thus, reduced *Ptk7* gene dosage may enhance the dominant effects of the *Looptail* mutation on neural tube closure. *Fz3/Fz6* genes have unique qualities among the noncanonical Wnt pathway components: *Fz3/Fz6* mutations cause bundle misorientation primarily in IHCs, where bundle orientation is frequently reversed. Furthermore, *Fz3/Fz6* and Dvl2 appear to localize to opposite poles of hair cells, which is at odds with a conserved role of Fz in Dishevelled recruitment through direct binding [45]. Thus, our results add to a growing body of evidence that suggests *Fz3/Fz6* use novel mechanisms to regulate hair cell PCP. We propose that *Fz3/Fz6* and *Ptk7* act in an opposing fashion to modulate actomyosin contractility in the OC and that reduced *Fz3* localization in the *Ptk7^{-/-}* OC is likely a secondary effect of altered actomyosin organization rather than the cause for bundle misorientation.

We show that *Ptk7* and the noncanonical Wnt pathway differentially regulate a contractile apical myosin II network in supporting cells. These structures are analogous to those observed during *Drosophila* gastrulation [46, 47] and germ band extension [48–50], which generate pulsed contractile forces near cell-cell junctions to drive apical constriction and cell intercalation, respectively. We hypothesize that the apical myosin II foci in supporting cells may engage in similar contractile behaviors to exert pulling forces on neighboring hair cells.

Ptk7 modulates myosin II-based contractile tension on hair cells by mediating the assembly of the apical myosin network in supporting cells. *Fz3/Fz6* may modulate contractility in hair cells and/or supporting cells to counterbalance the pulling forces on hair cells (Figure 7Q). In support of this model, we show that vinculin, a force-sensitive actin binding molecule, is normally enriched along the medial junctions of hair cells, that this planar asymmetry is lost in *Ptk7*^{-/-} mutants, and importantly, both vinculin planar asymmetry and bundle orientation were restored in *Fz3*^{-/-}; *Ptk7*^{-/-} double mutants.

The precise mechanisms by which PTK7 regulates myosin II activity remain to be determined. Paradoxically, in spite of reduced junctional myosin II staining, pRLC level was increased in *Ptk7*^{-/-} OC. Therefore, it is unlikely that PTK7 regulates myosin II activity through RLC phosphorylation *per se*. Different myosin II isoforms are regulated by distinct upstream signals [51]. *Ptk7*-deficiency affected the localization of all three heavy chain isoforms, with the strongest impact on MIIB, which has properties best suited to exert tension [33]. These results are consistent with a role of PTK7 in myosin II heavy chain regulation. We suspect that the increased level of pRLC in *Ptk7*^{-/-} OC may reflect a compensatory response to compromised myosin II heavy chain function.

How might contractile tension orient hair cell PCP? We showed previously that hair cell PCP is controlled by Rac-PAK signaling [4, 5]. Interestingly, several *in vitro* studies suggest that tension and myosin II can inhibit Rac activity through GEFs and GAPs for Rac [52–55]. Consistent with this idea, activated PAK and vinculin exhibit complementary patterns of planar asymmetry in hair cells. We propose that polarized contractile tension between OC epithelial cells regulates the spatial pattern of Rac-PAK activity to orient hair cell PCP (Figure 7Q).

Experimental Procedures

See Supplemental Experimental Procedures for complete methods.

Highlights

- *Ptk7* and *Fz3/Fz6* act in parallel and have opposing effects on hair cell PCP.
- Mosaic analysis indicates a requirement of *Ptk7* in supporting cells for hair cell PCP.
- *Ptk7* mediates the assembly of contractile apical myosin II foci in supporting cells.
- *Ptk7* promotes junctional planar asymmetry of vinculin, a tension-sensitive molecule.

Supplementary Material

Refer to Web version on PubMed Central for supplementary material.

Acknowledgments

We thank Drs. Paul Adler, Douglas DeSimone, Alan ‘Rick’ Horwitz, Raymond Keller, Martin Schwartz, Ann Sutherland and members of the Lu laboratory for helpful comments on the manuscript; Drs. Robert Adelstein and Matthew Kelley for *Myh10*^{DN} mice; and Drs. Jeremy Nathans and Yanshu Wang for Fz plasmids, antibodies and mice. This study was supported by a Basil O’Connor Starter Scholar Research Awards (#5-FY07-166) from the March of Dimes Foundation and the NIH grant R01 DC009238 (to X.L.). C.W.S. was supported by NIH training grant T32 GM008136 for Cell and Molecular Biology at the University of Virginia.

References

1. Schwander M, Kachar B, Muller U. Review series: The cell biology of hearing. *J Cell Biol.* 2010; 190:9–20. [PubMed: 20624897]
2. Goodrich LV, Strutt D. Principles of planar polarity in animal development. *Development.* 2011; 138:1877–1892. [PubMed: 21521735]
3. Rida PC, Chen P. Line up and listen: Planar cell polarity regulation in the mammalian inner ear. *Semin Cell Dev Biol.* 2009; 20:978–985. [PubMed: 19508855]
4. Grimsley-Myers CM, Sipe CW, Geleoc GS, Lu X. The small GTPase Rac1 regulates auditory hair cell morphogenesis. *J Neurosci.* 2009; 29:15859–15869. [PubMed: 20016102]
5. Sipe CW, Lu X. Kif3a regulates planar polarization of auditory hair cells through both ciliary and non-ciliary mechanisms. *Development.* 2011; 138:3441–3449. [PubMed: 21752934]
6. Yamamoto N, Okano T, Ma X, Adelstein RS, Kelley MW. Myosin II regulates extension, growth and patterning in the mammalian cochlear duct. *Development.* 2009; 136:1977–1986. [PubMed: 19439495]
7. Montcouquiol M, Rachel RA, Lanford PJ, Copeland NG, Jenkins NA, Kelley MW. Identification of Vangl2 and Scrb1 as planar polarity genes in mammals. *Nature.* 2003; 423:173–177. [PubMed: 12724779]
8. Lu X, Borchers AG, Jolicoeur C, Rayburn H, Baker JC, Tessier-Lavigne M. PTK7/CCK-4 is a novel regulator of planar cell polarity in vertebrates. *Nature.* 2004; 430:93–98. [PubMed: 15229603]
9. Narimatsu M, Bose R, Pye M, Zhang L, Miller B, Ching P, Sakuma R, Luga V, Roncari L, Attisano L, et al. Regulation of planar cell polarity by Smurf ubiquitin ligases. *Cell.* 2009; 137:295–307. [PubMed: 19379695]
10. Merte J, Jensen D, Wright K, Sarsfield S, Wang Y, Schekman R, Ginty DD. Sec24b selectively sorts Vangl2 to regulate planar cell polarity during neural tube closure. *Nat Cell Biol.* 2010; 12:41–46. sup pp 41–48. [PubMed: 19966784]
11. Wansleben C, Feitsma H, Montcouquiol M, Kroon C, Cuppen E, Meijlink F. Planar cell polarity defects and defective Vangl2 trafficking in mutants for the COPII gene Sec24b. *Development.* 2010; 137:1067–1073. [PubMed: 20215345]
12. Paudyal A, Damrau C, Patterson VL, Ermakov A, Formstone C, Lalanne Z, Wells S, Lu X, Norris DP, Dean CH, et al. The novel mouse mutant, chuzhoi, has disruption of Ptk7 protein and exhibits defects in neural tube, heart and lung development and abnormal planar cell polarity in the ear. *BMC Dev Biol.* 2010; 10:87. [PubMed: 20704721]
13. Shnitsar I, Borchers A. PTK7 recruits dsh to regulate neural crest migration. *Development.* 2008; 135:4015–4024. [PubMed: 19004858]
14. Wehner P, Shnitsar I, Urlaub H, Borchers A. RACK1 is a novel interaction partner of PTK7 that is required for neural tube closure. *Development.* 2011; 138:1321–1327. [PubMed: 21350015]
15. Yen WW, Williams M, Periasamy A, Conaway M, Burdsal C, Keller R, Lu X, Sutherland A. PTK7 is essential for polarized cell motility and convergent extension during mouse gastrulation. *Development.* 2009; 136:2039–2048. [PubMed: 19439496]
16. Adler PN. Planar signaling and morphogenesis in *Drosophila*. *Dev Cell.* 2002; 2:525–535. [PubMed: 12015961]
17. Axelrod JD. Unipolar membrane association of Dishevelled mediates Frizzled planar cell polarity signaling. *Genes Dev.* 2001; 15:1182–1187. [PubMed: 11358862]
18. Wang J, Mark S, Zhang X, Qian D, Yoo SJ, Radde-Gallwitz K, Zhang Y, Lin X, Collazo A, Wynshaw-Boris A, et al. Regulation of polarized extension and planar cell polarity in the cochlea by the vertebrate PCP pathway. *Nat Genet.* 2005; 37:980–985. [PubMed: 16116426]
19. Wang Y, Guo N, Nathans J. The role of Frizzled3 and Frizzled6 in neural tube closure and in the planar polarity of inner-ear sensory hair cells. *J Neurosci.* 2006; 26:2147–2156. [PubMed: 16495441]
20. Montcouquiol M, Sans N, Huss D, Kach J, Dickman JD, Forge A, Rachel RA, Copeland NG, Jenkins NA, Bogani D, et al. Asymmetric localization of Vangl2 and Fz3 indicate novel

- mechanisms for planar cell polarity in mammals. *J Neurosci.* 2006; 26:5265–5275. [PubMed: 16687519]
21. Hebert JM, McConnell SK. Targeting of cre to the Foxg1 (BF-1) locus mediates loxP recombination in the telencephalon and other developing head structures. *Dev Biol.* 2000; 222:296–306. [PubMed: 10837119]
 22. Lakso M, Pichel JG, Gorman JR, Sauer B, Okamoto Y, Lee E, Alt FW, Westphal H. Efficient in vivo manipulation of mouse genomic sequences at the zygote stage. *Proc Natl Acad Sci U S A.* 1996; 93:5860–5865. [PubMed: 8650183]
 23. Boutros M, Paricio N, Strutt DJ, Mlodzik M. Dishevelled activates JNK and discriminates between JNK pathways in planar polarity and wingless signaling. *Cell.* 1998; 94:109–118. [PubMed: 9674432]
 24. Yamanaka H, Moriguchi T, Masuyama N, Kusakabe M, Hanafusa H, Takada R, Takada S, Nishida E. JNK functions in the non-canonical Wnt pathway to regulate convergent extension movements in vertebrates. *EMBO Rep.* 2002; 3:69–75. [PubMed: 11751577]
 25. Dong C, Yang DD, Wysk M, Whitmarsh AJ, Davis RJ, Flavell RA. Defective T cell differentiation in the absence of Jnk1. *Science.* 1998; 282:2092–2095. [PubMed: 9851932]
 26. Kuan CY, Yang DD, Samanta Roy DR, Davis RJ, Rakic P, Flavell RA. The Jnk1 and Jnk2 protein kinases are required for regional specific apoptosis during early brain development. *Neuron.* 1999; 22:667–676. [PubMed: 10230788]
 27. Davis RJ. Signal transduction by the JNK group of MAP kinases. *Cell.* 2000; 103:239–252. [PubMed: 11057897]
 28. Winter CG, Wang B, Ballew A, Royou A, Karess R, Axelrod JD, Luo L. Drosophila Rho-associated kinase (Drok) links Frizzled-mediated planar cell polarity signaling to the actin cytoskeleton. *Cell.* 2001; 105:81–91. [PubMed: 11301004]
 29. Lee JY, Marston DJ, Walston T, Hardin J, Halberstadt A, Goldstein B. Wnt/Frizzled signaling controls *C. elegans* gastrulation by activating actomyosin contractility. *Curr Biol.* 2006; 16:1986–1997. [PubMed: 17055977]
 30. Conti MA, Adelstein RS. Nonmuscle myosin II moves in new directions. *J Cell Sci.* 2008; 121:11–18. [PubMed: 18096687]
 31. Skoglund P, Rolo A, Chen X, Gumbiner BM, Keller R. Convergence and extension at gastrulation require a myosin IIB-dependent cortical actin network. *Development.* 2008; 135:2435–2444. [PubMed: 18550716]
 32. Rolo A, Skoglund P, Keller R. Morphogenetic movements driving neural tube closure in *Xenopus* require myosin IIB. *Dev Biol.* 2009; 327:327–338. [PubMed: 19121300]
 33. Vicente-Manzanares M, Ma X, Adelstein RS, Horwitz AR. Non-muscle myosin II takes centre stage in cell adhesion and migration. *Nat Rev Mol Cell Biol.* 2009; 10:778–790. [PubMed: 19851336]
 34. Ma X, Bao J, Adelstein RS. Loss of cell adhesion causes hydrocephalus in nonmuscle myosin II-B-ablated and mutated mice. *Mol Biol Cell.* 2007; 18:2305–2312. [PubMed: 17429076]
 35. Peng X, Nelson ES, Maiers JL, DeMali KA. New insights into vinculin function and regulation. *Int Rev Cell Mol Biol.* 2011; 287:191–231. [PubMed: 21414589]
 36. Hoffman BD, Grashoff C, Schwartz MA. Dynamic molecular processes mediate cellular mechanotransduction. *Nature.* 2011; 475:316–323. [PubMed: 21776077]
 37. Gomez GA, McLachlan RW, Yap AS. Productive tension: force-sensing and homeostasis of cell-cell junctions. *Trends Cell Biol.* 2011; 21:499–505. [PubMed: 21763139]
 38. Pasapera AM, Schneider IC, Rericha E, Schlaepfer DD, Waterman CM. Myosin II activity regulates vinculin recruitment to focal adhesions through FAK-mediated paxillin phosphorylation. *J Cell Biol.* 2010; 188:877–890. [PubMed: 20308429]
 39. Grashoff C, Hoffman BD, Brenner MD, Zhou R, Parsons M, Yang MT, McLean MA, Sligar SG, Chen CS, Ha T, et al. Measuring mechanical tension across vinculin reveals regulation of focal adhesion dynamics. *Nature.* 2010; 466:263–266. [PubMed: 20613844]
 40. Yonemura S, Wada Y, Watanabe T, Nagafuchi A, Shibata M. alpha-Catenin as a tension transducer that induces adherens junction development. *Nat Cell Biol.* 2010; 12:533–542. [PubMed: 20453849]

41. le Duc Q, Shi Q, Blonk I, Sonnenberg A, Wang N, Leckband D, de Rooij J. Vinculin potentiates E-cadherin mechanosensing and is recruited to actin-anchored sites within adherens junctions in a myosin II-dependent manner. *J Cell Biol.* 2010; 189:1107–1115. [PubMed: 20584916]
42. Kibar Z, Salem S, Bosoi CM, Pauwels E, De Marco P, Merello E, Bassuk AG, Capra V, Gros P. Contribution of VANGL2 mutations to isolated neural tube defects. *Clin Genet.* 2010; 80:76–82. [PubMed: 20738329]
43. Guyot MC, Bosoi CM, Kharfallah F, Reynolds A, Drapeau P, Justice M, Gros P, Kibar Z. A novel hypomorphic Looptail allele at the planar cell polarity Vangl2 gene. *Dev Dyn.* 2011; 240:839–849. [PubMed: 21404367]
44. Yin H, Copley CO, Goodrich LV, Deans MR. Comparison of Phenotypes between Different vangl2 Mutants Demonstrates Dominant Effects of the Looptail Mutation during Hair Cell Development. *PLoS One.* 2012; 7:e31988. [PubMed: 22363783]
45. Wong HC, Bourdelas A, Krauss A, Lee HJ, Shao Y, Wu D, Mlodzik M, Shi DL, Zheng J. Direct binding of the PDZ domain of Dishevelled to a conserved internal sequence in the C-terminal region of Frizzled. *Mol Cell.* 2003; 12:1251–1260. [PubMed: 14636582]
46. Martin AC, Kaschube M, Wieschaus EF. Pulsed contractions of an actin-myosin network drive apical constriction. *Nature.* 2009; 457:495–499. [PubMed: 19029882]
47. Martin AC, Gelbart M, Fernandez-Gonzalez R, Kaschube M, Wieschaus EF. Integration of contractile forces during tissue invagination. *J Cell Biol.* 2010; 188:735–749. [PubMed: 20194639]
48. Rauzi M, Lenne PF, Lecuit T. Planar polarized actomyosin contractile flows control epithelial junction remodelling. *Nature.* 2010; 468:1110–1114. [PubMed: 21068726]
49. Fernandez-Gonzalez R, Zallen JA. Oscillatory behaviors and hierarchical assembly of contractile structures in intercalating cells. *Phys Biol.* 2011; 8:045005. [PubMed: 21750365]
50. Sawyer JK, Choi W, Jung KC, He L, Harris NJ, Peifer M. A contractile actomyosin network linked to adherens junctions by Canoe/afadin helps drive convergent extension. *Mol Biol Cell.* 2011; 22:2491–2508. [PubMed: 21613546]
51. Smutny M, Cox HL, Leerberg JM, Kovacs EM, Conti MA, Ferguson C, Hamilton NA, Parton RG, Adelstein RS, Yap AS. Myosin II isoforms identify distinct functional modules that support integrity of the epithelial zonula adherens. *Nat Cell Biol.* 2010; 12:696–702. [PubMed: 20543839]
52. Katsumi A, Milanini J, Kiosses WB, del Pozo MA, Kaunas R, Chien S, Hahn KM, Schwartz MA. Effects of cell tension on the small GTPase Rac. *J Cell Biol.* 2002; 158:153–164. [PubMed: 12105187]
53. Lee CS, Choi CK, Shin EY, Schwartz MA, Kim EG. Myosin II directly binds and inhibits Dbl family guanine nucleotide exchange factors: a possible link to Rho family GTPases. *J Cell Biol.* 2010; 190:663–674. [PubMed: 20713598]
54. Even-Ram S, Doyle AD, Conti MA, Matsumoto K, Adelstein RS, Yamada KM. Myosin IIA regulates cell motility and actomyosin-microtubule crosstalk. *Nat Cell Biol.* 2007; 9:299–309. [PubMed: 17310241]
55. Ehrlicher AJ, Nakamura F, Hartwig JH, Weitz DA, Stossel TP. Mechanical strain in actin networks regulates FilGAP and integrin binding to filamin A. *Nature.* 2011; 478:260–263. [PubMed: 21926999]

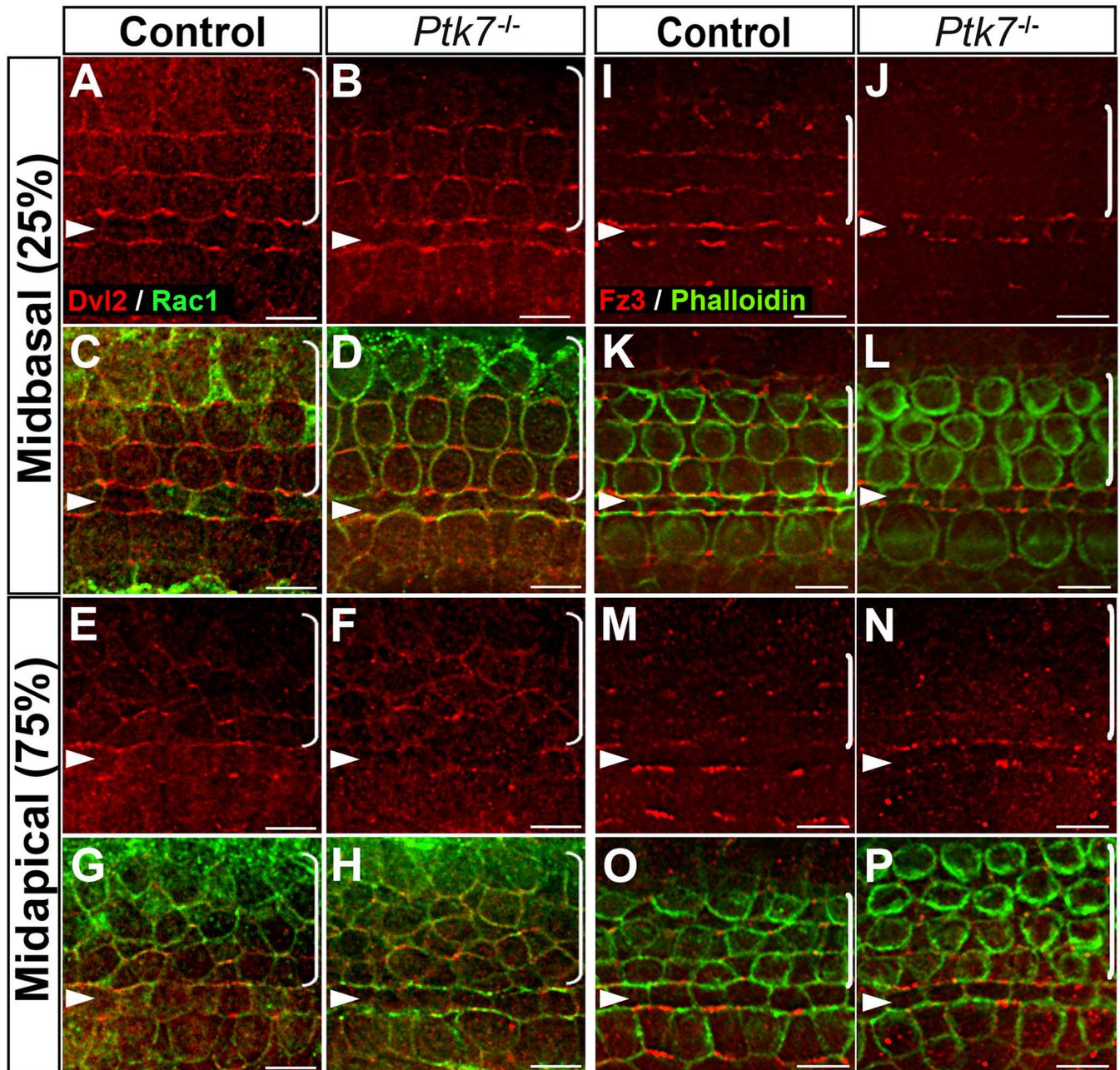


Figure 1. *Ptk7* regulates *Fz3* localization but is not required for asymmetric localization of *Dvl2* in the OC

(A–D) In the mid-basal region of the OC at E17.5, *Dvl2* (red) was enriched on the lateral membranes of hair cells in both control (A, C) and *Ptk7*^{-/-} cochleae (B, D). (E–H) In the mid-apical region of the OC at E17.5, similar membrane localization of *Dvl2* was observed in control (E, G) and *Ptk7*^{-/-} cochlea (F, H). Cell boundaries were labeled with *Rac1* immunostaining (green). (I–L) In the mid-basal region of OC at E17.5, *Fz3* (red) was enriched on the medial membranes of hair cells and supporting cells in control (I, K). This localization was disrupted in *Ptk7*^{-/-} cochleae (J, L). (M–P) In the mid-apical region of the OC at E17.5, asymmetric localization of *Fz3* was not apparent in either control (M, O) or *Ptk7*^{-/-} cochleae (N, P). Green, phalloidin staining. Percentages indicate the distance of the

positions analyzed from the base relative to the length of the cochlea. Arrowheads indicate the row of pillar cells. Brackets indicate OHC rows. Lateral is up in all micrographs. Scale bar: 6 μm . (See also Figure S1).

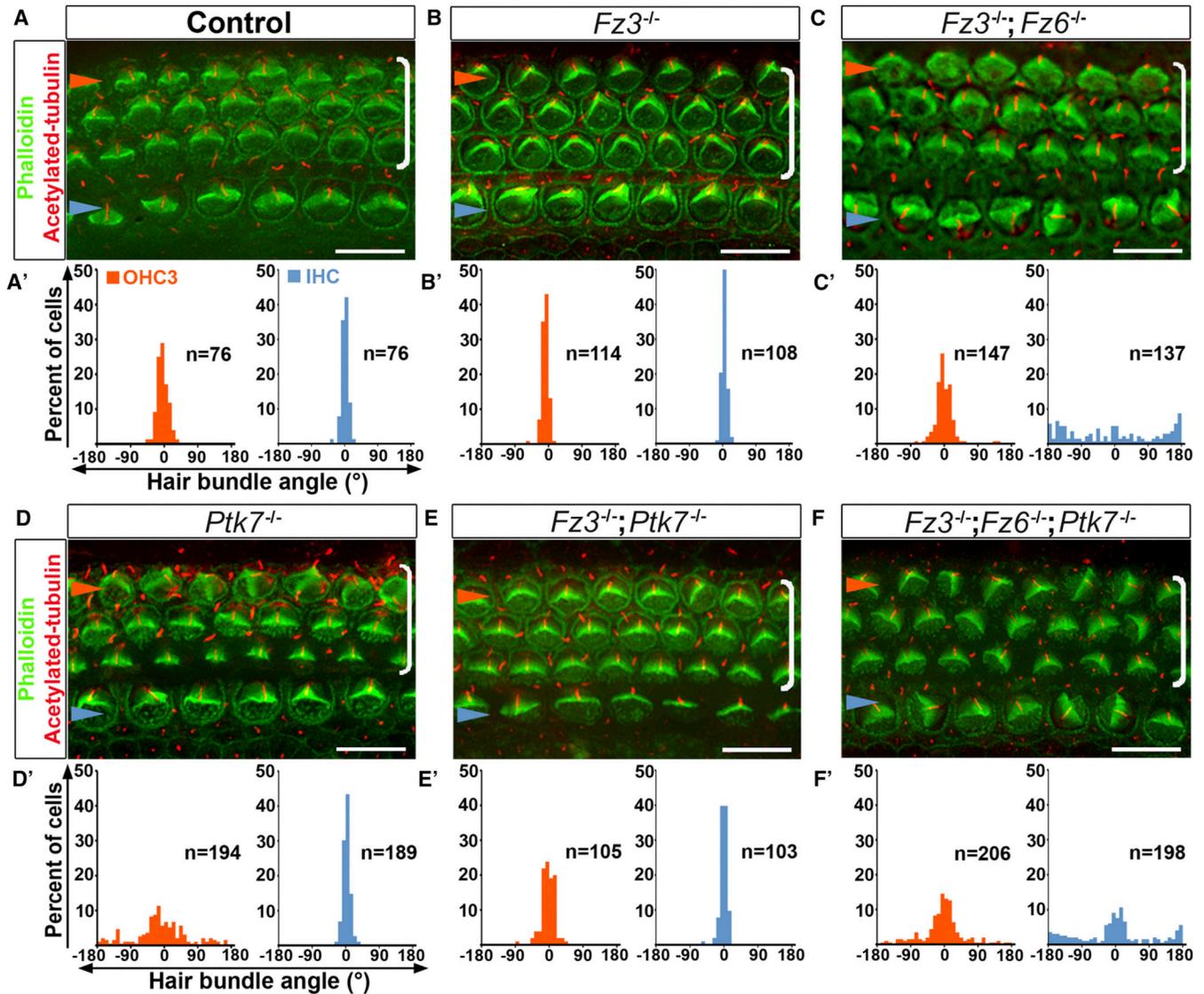


Figure 2. Epistasis analysis of *Ptk7* and *Fz3/Fz6* in hair cell PCP

(A–F) Basal region (15% cochlear length) of E18.5 cochleae stained with phalloidin (green) and acetylated tubulin (red) to visualize the stereocilia and the kinocilium, respectively. Genotypes are indicated above the panels. (A'–F') Quantification of bundle orientation in OHC3 (orange bars) and IHC (blue bars) rows for the indicated genotypes. In control (A, A') and *Fz3*^{-/-} cochleae (B, B'), OHC3 and IHC bundle orientation do not deviate beyond 30° from the medial-lateral axis. (C, C') In *Fz3*^{-/-}; *Fz6*^{-/-} mutants, the bundle orientation defect was most pronounced in IHCs. (D, D') In *Ptk7*^{-/-} mutants, bundle orientation defects were most pronounced in OHC3s. (E, E') In *Fz3*^{-/-}; *Ptk7*^{-/-} mutants, bundle orientation in OHC3s was significantly improved compared to *Ptk7*^{-/-} mutants. (F, F') *Fz3*^{-/-}; *Fz6*^{-/-}; *Ptk7*^{-/-} triple mutants displayed an additive defect in bundle orientation. Blue arrowheads indicate the row of IHCs, orange arrowheads indicate the OHC3 row and brackets indicate all OHC rows. Lateral is up in all micrographs. Scale bar: 10 μm. (See also Figure S2).

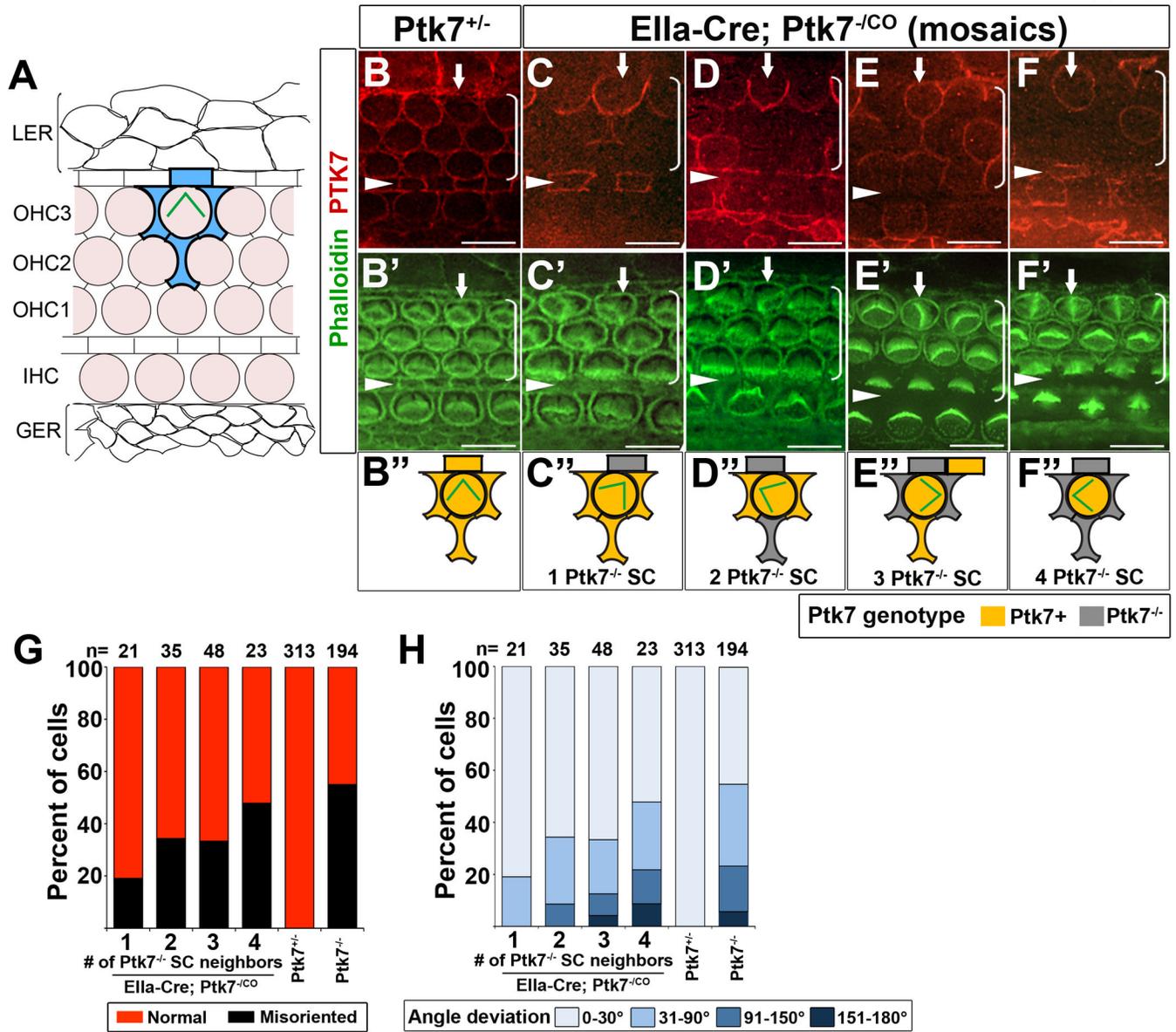


Figure 3. Mosaic analysis of Ptk7 in hair cell PCP

(A) Schematic diagram of cellular organization in the OC. Hair cells (shaded light pink) are separated from one another by intervening supporting cells. Each hair cell in OHC3 is immediately surrounded by four supporting cells (shaded in blue). Flanking the OC are cells of the lesser epithelial ridge (LER) and the greater epithelial ridge (GER). (B-F'') Mid-basal region (25% cochlear length) of E18.5 cochleae stained with PTK7 antibodies (red) and phalloidin (green). (B, B') In controls, PTK7 is expressed in both hair cells and supporting cells and localized to cell-cell contacts. (C-F'') Examples of Ptk7 mosaics in E11a-Cre; Ptk7^{-ICO} cochleae. Ptk7⁺ hair cells with misoriented stereociliary bundles (arrows) surrounded by different numbers of Ptk7^{-/-} supporting cells (SC) are shown and schematized. (G, H) In E11a-Cre; Ptk7^{-ICO} mosaic cochleae, both the penetrance (G) and the severity (H) of bundle orientation defects in Ptk7⁺ OHC3 positively correlates with the number of Ptk7^{-/-} supporting cell neighbors. Arrowheads indicate the row of pillar cells.

Brackets indicate OHC rows. Lateral is up in all micrographs. Scale bar: 10 μm . (See also Figure S3).

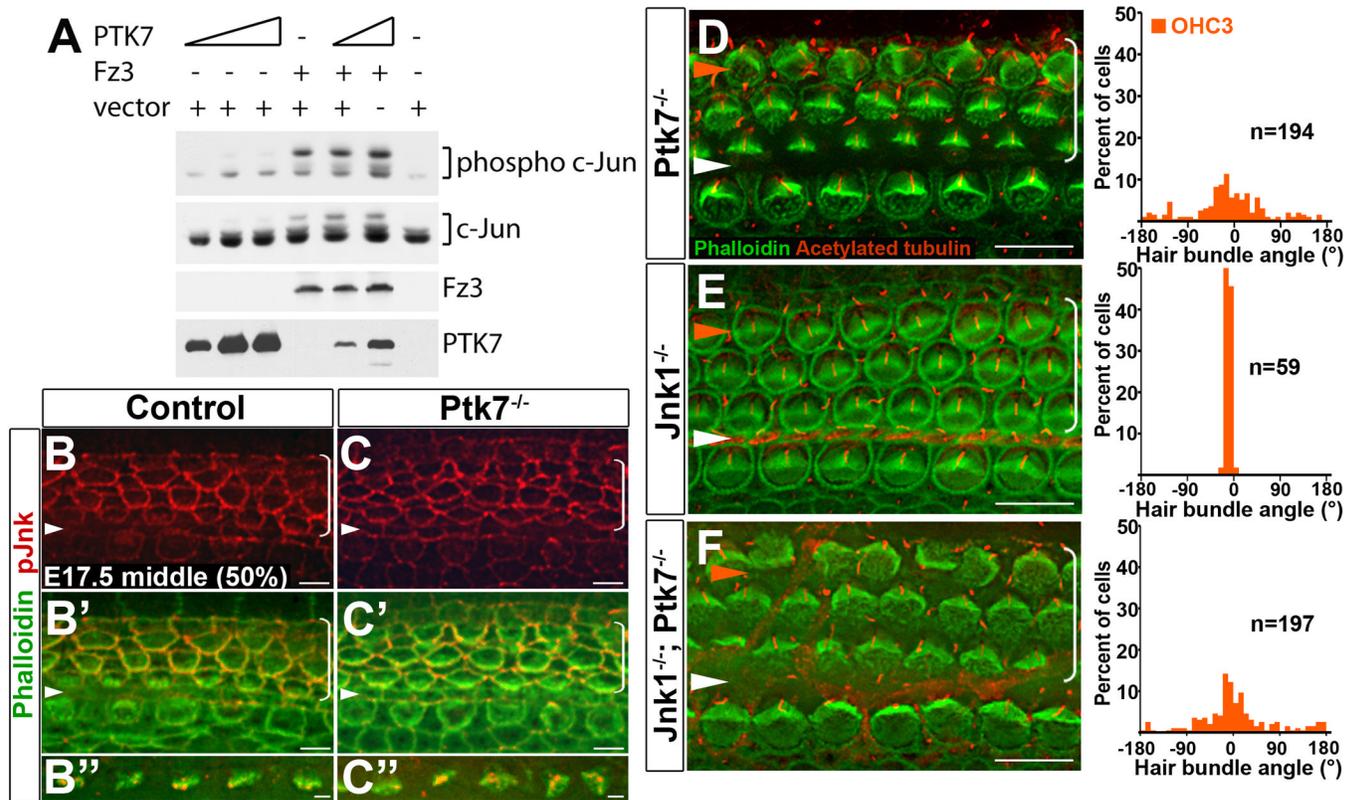


Figure 4. JNK signaling is unlikely to mediate PTK7 function in the OC

(A) PTK7 expression has no effect on JNK activation *in vitro*. HEK293T cells were transfected either with PTK7, Fz3 or both and assayed for c-Jun phosphorylation. (B–C'') In the middle turn of E17.5 OC (50% cochlear length), pJNK localization (red) in the Ptk7^{-/-} OC (C–C'') was similar to the control (B–B''). Green, phalloidin staining. (D–F) Basal region (15% cochlear length) of E18.5 Ptk7^{-/-} (D), Jnk1^{-/-} (E) and Jnk1^{-/-}; Ptk7^{-/-} (F) cochleae stained with phalloidin (green) and acetylated tubulin (red). Quantifications of bundle orientation of OHC3s are shown to the right. White arrowheads indicate the row of pillar cells; orange arrowheads indicate the OHC3 row. Brackets indicate OHC rows. Lateral is up in all micrographs. Scale bars, B–C', 6 μ m; B'', C'', 2 μ m; D–F, 10 μ m.

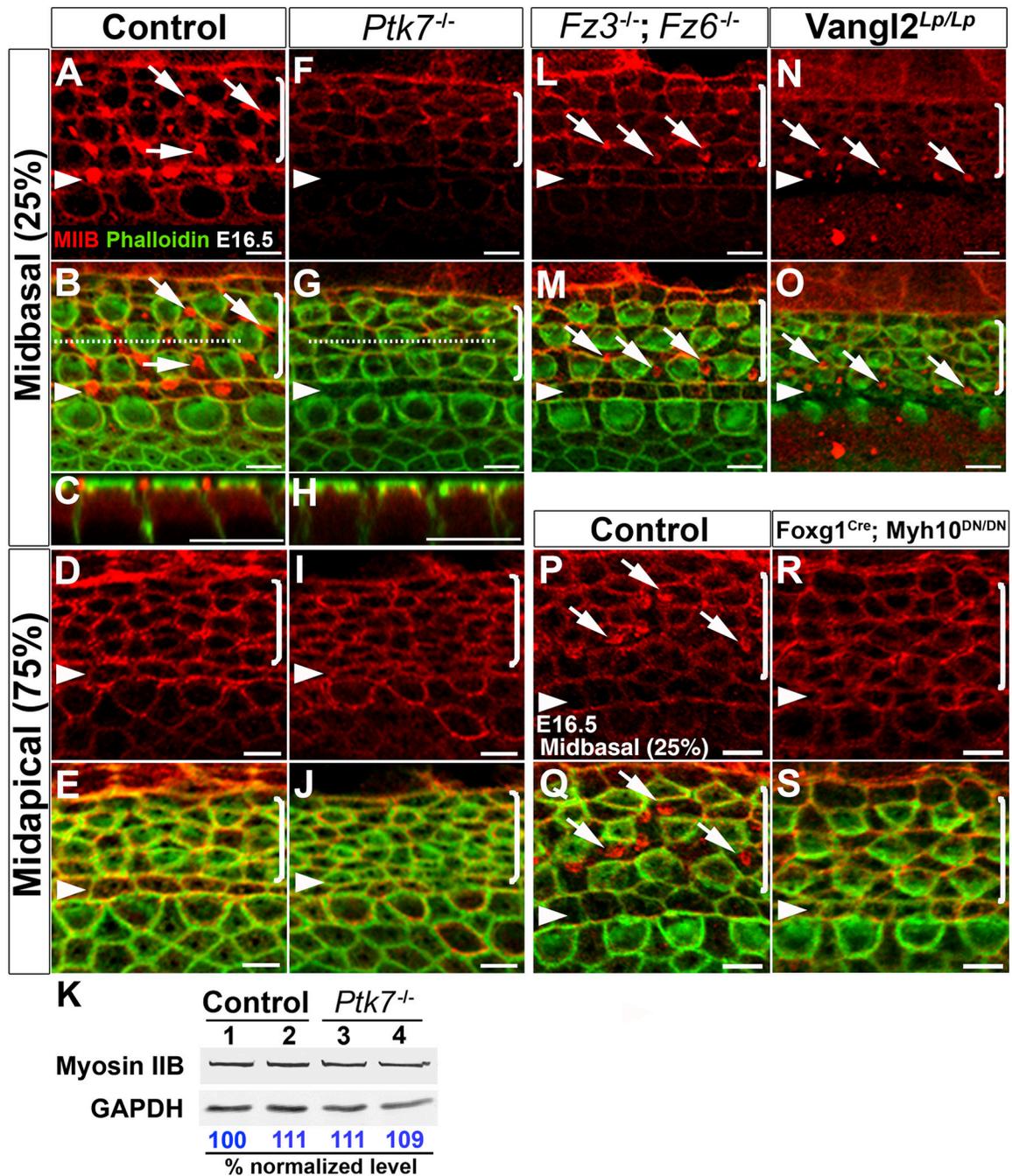
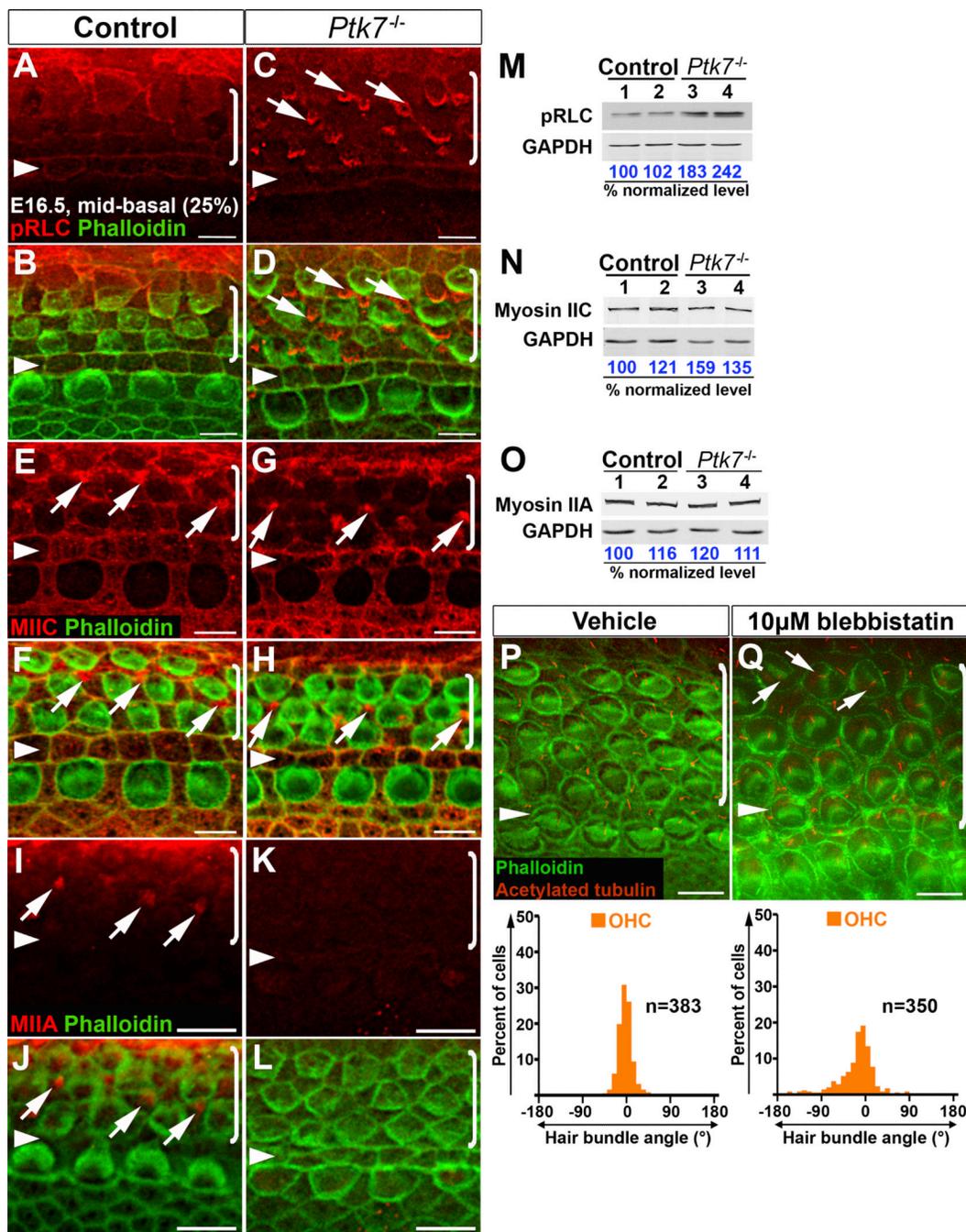


Figure 5. PTK7 and the noncanonical Wnt pathway differentially regulate a contractile myosin IIB network in supporting cells

(A–J, L–S) Confocal images of MIIB (red) and phalloidin (green) staining in the OC at E16.5. (A–E) In the control OC, MIIB is localized to cell-cell contacts and to apical foci in the supporting cells in the mid-basal region of the OC (A–C). (F–J) In *Ptk7*^{-/-} OC, apical MIIB foci were absent from supporting cells (F–H) and overall junctional MIIB staining was reduced. (C, H) Z projections along the dashed lines in B and G, respectively, showing the apical position of the MIIB foci in supporting cells. (K) Total levels of MIIB in E16.5 *Ptk7*^{-/-} cochleae were comparable to controls. Lysates from four cochleae of the same genotype were pooled and loaded in each lane. GAPDH served as loading control. Numbers

on the bottom indicate percentage of normalized levels. (L–O) Apical MIIB foci (arrows) were still present in the supporting cells of $Fz3^{-/-}$; $Fz6^{-/-}$ (L, M) and $Vangl2^{Lp/Lp}$ (N, O) mutants, albeit smaller in size. (P–Q) Wild-type MIIB is localized to cell-cell contacts and apical foci in supporting cells (arrows). (R–S) ATPase-deficient MIIB (R709C) was localized to cell-cell contacts but failed to assemble into apical foci in supporting cells. Percentages indicate the distance of the positions analyzed from the base relative to the length of the cochlea. Arrowheads indicate the row of pillar cells. Brackets indicate OHC rows. Lateral is up in all micrographs. Scale bars, A–J, L–S, 5 μm .



Lysates from four cochleae of the same genotype were pooled and loaded in each lane. GAPDH served as loading control. Numbers on the bottom indicate percentage of normalized levels. (P, Q) Phalloidin (green) and acetylated-tubulin (red) staining of cochlear explants treated with either vehicle (P) or 10 μ M blebbistatin (Q), with quantification of bundle orientation shown beneath. Arrows indicate examples of misoriented stereociliary bundles in blebbistatin-treated explants. Arrowheads indicate the row of pillar cells. Brackets indicate OHC rows. Lateral is up in all micrographs. Scale bars, A–H, 5 μ m; I–L, P–Q, 6 μ m.

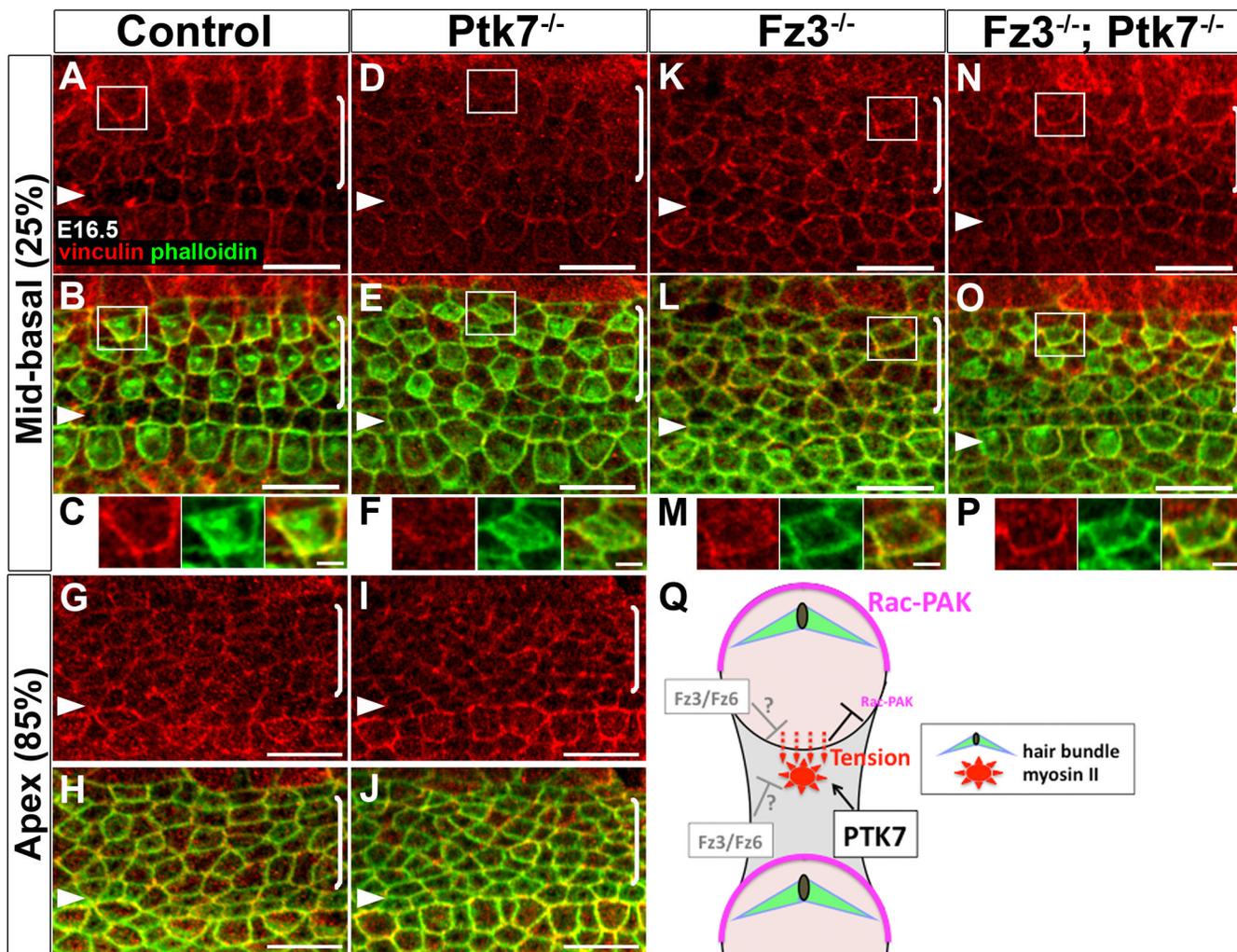


Figure 7. Planar asymmetry of junctional vinculin is abolished in Ptk7^{-/-} OC and restored in Fz3^{-/-}; Ptk7^{-/-} OC

(A–P) Confocal images of vinculin (red) and phalloidin (green) staining at E16.5. (A–C) In the mid-basal region (25% cochlear length) of control OC, vinculin was asymmetrically localized along cell-cell junctions and enriched on the medial side of hair cell membranes. (D–F) In the mid-basal region of Ptk7^{-/-} OC, junctional vinculin localization lost planar asymmetry and was greatly reduced compared to controls. (G–J) In the apex (85% cochlear length), junctional vinculin staining in the control (G, H) and Ptk7^{-/-} OC (I, J) was similar, with no apparent planar asymmetry. (K–M) In the mid-basal region of Fz3^{-/-} OC, junctional vinculin staining was similar to controls but its planar asymmetry was less robust. (N–P) In the mid-basal region of the Fz3^{-/-}; Ptk7^{-/-} OC, planar asymmetry of junctional vinculin was restored. (C, F, M, P) High magnification of the boxed hair cell above. Lateral is up in all micrographs. Scale bars, C, F, M, P, 2 μ m; other panels, 10 μ m. (Q) A proposed model for regulation of hair cell PCP by Ptk7. Acting in supporting cells (shaded grey), Ptk7 mediates the assembly of a contractile apical myosin II network to exert pulling forces on the medial border of hair cells, leading to enhanced contractile tension as evidenced by increased vinculin recruitment. In turn, polarized contractile tension promotes asymmetric Rac-PAK activity on the lateral side of hair cell cortex (shown in magenta) to orient the stereocilia

bundle. *Fz3/Fz6* may act in hair cells and/or supporting cells to counterbalance *Ptk7*-mediated contractile tension on hair cells. (See also Figure S4).